Liquefaction potential of sand-gravel mixtures: experimental observations

A. Pokhrel, G. Chiaro, M. Cubrinovski
University of Canterbury, Christchurch

T. Kiyota
Institute of Industrial Science, University of Tokyo, Japan

ABSTRACT

Case histories from at least 27 earthquakes worldwide (including three from New Zealand: 1929 M_w7.6 Murchison earthquake; 2010 M_w 7.1 Darfield earthquake; and 2016 M_w 7.8 Kaikoura earthquake) have indicated that liquefaction can occur in gravelly soils (both in natural deposits and manmade reclamations) inducing large ground deformation and causing severe damage to civil infrastructures. However, the evaluation of the liquefaction potential and deformation characteristics of gravelly soils remains to be a major challenge in geotechnical earthquake engineering. Aimed at providing new and useful insights on this important topic, in this study, a series of undrained cyclic triaxial tests were conducted on selected sand-gravel mixtures (SGMs), which were attained by varying the proportion by weight of a fine sand (New Brighton sand), a coarse sand (washed river sand) and a rounded pea gravel. Reconstituted specimens (height = 130 mm and diameter = 61 mm) were prepared at two relative density states of 25% and 45% by wet tamping method. Fully saturated specimens were then isotopically consolidated at 100 kPa confining pressure and subjected to cyclic stress ratio (*CSR*) levels ranging between 0.15 and 0.45. In this paper, preliminary results are presented and discussed in terms of effects density state – i.e., relative density (D_r), and inter-granular void ratios – and gravel content (G_C), on the liquefaction potential of SGMs. It is shown that while the liquefaction potential tends to increase with both increasing D_r and G_C, it can be more uniquely described by the equivalent void ratio that accounts simultaneously for both the density state and gravel content effects.

1 INTRODUCTION

Gravelly soils are usually considered less susceptible to liquefaction than sandy soils. However, to date, at least 27 case histories of gravelly soil liquefaction have been reported worldwide (including three from New Zealand: 1929 M_w7.6 Murchison earthquake (Berrill et al. 1988); 2010 M_w7.1 Darfield earthquake

(Cubrinovski et al. 2010) and 2016 M_w7.8 Kaikoura earthquake (Cubrinovski et al. 2017)). The reported liquefied gravelly soils are mostly well-graded mixtures of sand and gravel.

Gravelly soils are often referred to as 'problematic' because their behaviour is poorly understood. The current engineering practice of evaluating the liquefaction performance of gravelly soils relies on the assumption that liquefiable gravelly soils behave similarly to the sandy ones. However, existing assessment procedures for sand may not work for gravelly soils and could be misleading engineering assessments because the micromechanical structures of such soils depend on the amount and type of sand and gravel present in the gravelly soils. Therefore, research in studying the liquefaction mechanism and developing proper analysis techniques for gravelly soils remains to be a crucial subject of study to minimize the damage and loss caused by the liquefaction of saturated gravelly soils in expected future events.

Past laboratory studies suggest that the liquefaction behaviour of gravelly soils is significantly affected by the relative density (D_r) and gravel content (G_C). However, available test results appear inconclusive and/or contradictory regarding the effect of G_C on the liquefaction resistance of gravelly soils (Chen et al. 2018). For example, Evans and Zhou (1995) reported that the liquefaction resistance (defined as 5% double amplitude shear strain in 10 cycle of loading) of SGMs having D_r = 40% increased from 0.15 to 0.32 with increasing G_C from 0% to 60%. On the other hand, Amini and Chakravrty (2003) noted that the liquefaction resistance of SGMs having D_r = 50% is in the range of 0.2 to 0.25 for G_C between 0 to 70%. This is probably due to the different grading properties of sand and gravel employed and compositional characteristics of mixtures formed during specimen preparation stages.

Laboratory data from similar studies also confirmed that the liquefaction resistance of gravelly soils is significantly influenced by the D_r. Kokusho et al. (2004) found a unique relationship between the global relative density and liquefaction resistance (defined as 5% double amplitude shear strain in 10 and 20 cycle of loading) of gravelly soils regardless of the particle gradation. However, the characterisation of mechanical behaviour of mixed soils using the global relative density or void ratio parameter is rarely perfect due to the random variation of density depending on sand and gravel content (Mitchell and Soga 1994). The application of well-established cyclic resistance ratio (CRR) – D_r relation developed based on clean sand is not straightforward to evaluate the liquefaction potential of any soils other than clean sand (Cubrinovski 2019). Therefore, inter-grain state framework concepts such as equivalent fraction density model (Evans and Zhou, 1995), equivalent void ratio (Thevanayagam 2007), skeleton void ratio (Chang et al. 2014) have been used to account for the combined effect of G_C and D_r on the liquefaction potential of SGMs, but additional and consistent data are needed to establish if a unique and robust framework can be developed or not.

Further laboratory studies are, therefore, necessary to provide better insights regarding the combined effects of G_C and D_r on the liquefaction behaviour of gravelly soils, and to establish an appropriate liquefaction evaluation framework for SGMs based on index and/or state parameters. This is addressed in this study.

2 LITERATURE REVIEW ON INTERGRAIN STATE CONCEPT

2.1 Threshold sand content

Depending on the presence of the amount of sand content (S_C), SGMs can be divided into sand and gravel dominated microstructures as shown in the schematic diagram in Figure 1. The S_C that divides sand and gravel dominated zone is defined as a threshold sand content ($S_{C(th)}$)(Chang and Phantachang 2016). Rahman et al. (2009) developed a semi-empirical equation to calculate the threshold fine content of sand-silt mixtures. Similarly, the $S_{C(th)}$ for SGMs can also be estimated adopting the concept proposed (Rahman et al. 2009) for the sand-silt mixtures as expressed by Eqn. (1):

$$S_{C(th)} = 0.4\left(\frac{1}{1+exp^{0\cdot5-\frac{0.13}{r}}}+r\right) \quad (1)$$

where r is (d_{50} / D_{10}), d_{50} = mean diameter of sand, D_{10} = 10% of gravel particles finer than D_{10}.

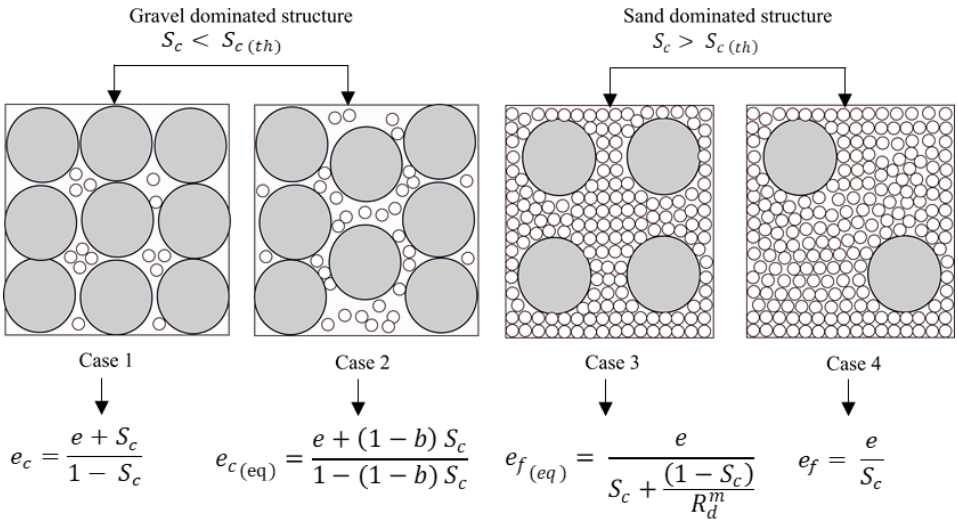

Figure 1 Schematic diagrams of microstructure of mixed soils (After Thevanagayam, 2007)

2.2 Skeleton Void Ratio

The void ratio for gravel and sand dominated structures can be described by the inter-grain state concept using a similar approach proposed by Thevanayagam (1998) for sand–silt mixtures. The void ratio for gravel dominated zone, where sand particles remain inactive without contributing to the mechanical response of the mixtures, is called gravel skeleton void ratio (e_c^*). It considers the sand content as void spaces in the mixtures and can be estimated by using Eqn. (2). Alternatively, the sand skeleton void ratio (e_f^*) represents the case where gravel particles are dispersed in a sand matrix and do not influence the sand particle force chain network. If the effect of gravel particles is ignored the resulting e_f^* can be estimated by Eqn. (3).

$$e_c^* = \frac{e + S_C}{1 - S_C} \quad (2)$$

$$e_f^* = \frac{e}{S_C} \quad (3)$$

where e is the global void ratio and S_C is the sand content.

The above concept ignores the effect on the load transfer mechanisms of sand particles in the gravel dominated zone and of gravel particles in the sand dominated zone. But the mechanical response of the mixtures is expected to be stronger than the host gravel matrix at the same e_c^* and host sand matrix at the same e_f^* (Thevanayagam 2007).

2.3 Equivalent Void Ratio

Even in the gravel dominated zone, where S_C is lower than $S_{C(th)}$, some of the sand particles support the gravel particles and take part in the force chain network as schematically described in the case 2 in Figure 1.

To account for the contribution of sand grains to the load transmission, Thevanayagam (2000) introduced the equivalent intergranular void ratio ($e_{c(eq)}$) that is defined by Eqn. (4).

$$e_{c(eq)} = \frac{e + (1-b)S_c}{1-(1-b)S_c} \tag{4}$$

where, b is the finer fraction that contributes to the coarse grain force chain network, and is influenced by the particle size disparity ratio (R_d). Rahman et al. (2008) proposed the semi-empirical expression in Eqn. (5) to predict the b value based on fine content and particle size.

$$b = \left[I - \exp\left(-0 \cdot 3 \frac{\left(\frac{S_c}{S_{C(th)}}\right)}{1 - r^{0 \cdot 25}}\right)\right]\left(r \frac{S_C}{S_{C(th)}}\right)^r \tag{5}$$

Similarly, when S_C is higher than $S_{C(th)}$, Thevanayagam (2007) hypothesized that the contribution of coarse particles to the fine grain force chain network cannot be completely neglected because coarse particles act as embedded reinforcement elements within the finer particles matrix until the limiting fine content $S_{C(lim)}$. Beyond the $S_{C(lim)}$, coarse particles are separated sufficiently without altering the behaviour of the finer matrix. The equivalent intergranular void ratio $e_{f(eq)}$ and limiting $S_{C(lim)}$ can be calculated from Eqns. (6) and (7), respectively:

$$e_{f(eq)} = \frac{e}{S_C + \frac{(1-S_C)}{R_d^m}} \tag{6}$$

$$S_{C(lim)} = \left[1 - \frac{\pi(1+e)}{6S^3}\right] \tag{7}$$

where R_d is the particle disparity ratio ($= D_{50} \,/\, d_{50}$), D_{50} is the mean diameter of gravel particles, d_{50} is mean diameter of sand particles, m is a fitting parameter which depends on the particle gradation and packing condition, and $S = 1 + (10 \,/\, R_d)$.

It should be noted that these equations were originally developed for sand–silt mixtures. Yet, considering that the binary packing condition for sand and gravel mixtures, as per this study, are analogous to the silt and sand of previous studies, all the above equations have been re-written in this paper for SGMs.

This study envisaged the four cases of microstructures schematically depicted in Figure 1 to define the skeleton and equivalent void ratio. However, eventually the laboratory study was carried out only focusing on sand dominated structures, i.e. Case 3 and Case 4 of Figure 1 – this is because for SGMs with $S_C < 60\%$ (i.e., Gc > 40%) segregation between small sand and large gravel particles could not be prevented, compromising the test repeatability and affecting the overall quality of the test results:

- Case 3:- gravel particles acts as an embedded reinforcement element and take part in stress transmission;
- Case 4:- gravel particles are separated sufficiently without playing any role to the sand matrix force chain network.

Please note that Case 3 and Case 4 are identical to Case iv-1 and iv-2 of Thevanayagam (2007).

3 TEST MATERIALS AND PROCEDURE

3.1 Test Materials

In this study two clean sands – namely New Brighton sand (NB sand; D_{50} = 0.2 mm; D_{max} = 0.425 mm; G_s = 2.67) and Dalton River Washed Sand (DRW sand, D_{50} = 0.75 mm; D_{max} = 3.5 mm; G_s = 2.67) – and a rounded pea gravel (D_{50} = 5.5 mm; D_{max} = 8 mm; G_s = 2.66) were used to prepare a variety of SGM specimens to be tested in the laboratory. The NB sand and DRW sand were firstly mixed in equal proportion by weight (50:50) to create a well-graded host sand. Then the pea gravel was added to generate the desired SGMs. Figure 2 shows the photographic images of the parent materials, and particle size distribution curves of the parent materials and four selected SGMs (with Gc content of 0, 10, 25 and 40% by mass) used to investigate the liquefaction behaviour of SGMs.

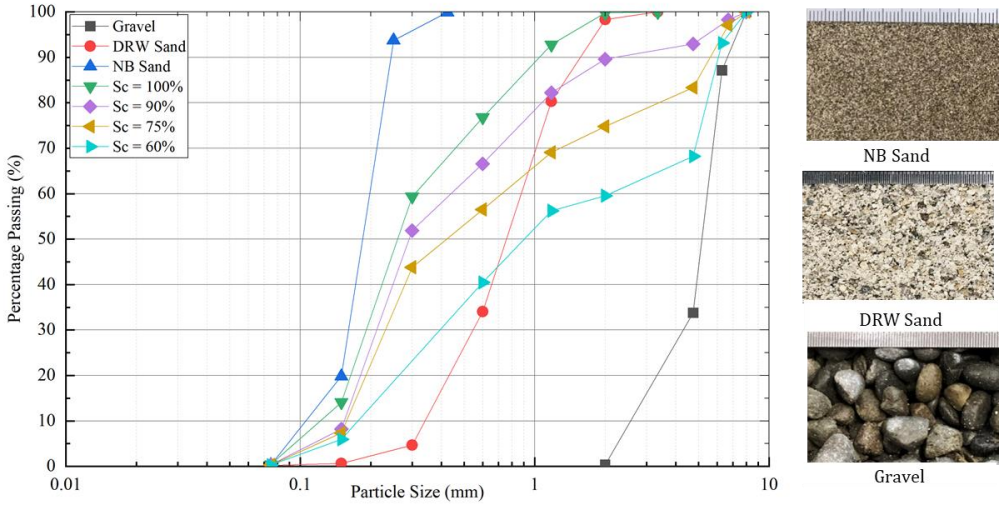

Figure 2 Particle size distribution curves of SGMs and photographic images of parent materials

Figure 3 shows the diagram of microstructure derived for the tested SGMs. In the plot, the values of the maximum and minimum void ratios were obtained experimentally in accordance to JGS 0162-2009. It can be seen that the $S_{C(th)}$ value is 31%.

As mentioned before, Case 3 and Case 4 are identical to Case iv-1 and iv-2 of (Thevanayagam 2007). More specifically, in this study, the mixtures with S_C = 0% and 10% represent Case 3, and those with S_C = 25% and 40% describe Case 4.

3.2 Specimen Preparation and testing procedure

A number of SGM specimens with height of 130 mm and diameter of 61 mm were prepared by using the wet tamping method. Firstly, the required mass of each material was calculated based on their dry density and the specimen size/volume. The materials were then divided into 5 equal parts to obtain homogeneous specimens with uniform particle size distribution and amount of each material. The preweighed oven-dry host sands and gravel were mixed with deaired water with a water content of 5% as recommended by Ishihara (1993). Then, the moist SGMs were compacted inside a split mould by means of a small compacting rod into 5 layers in case of loose specimen (i.e., D_r = 25%) and 10 layers for medium dense specimen (i.e., D_r = 45%). The compacting energy was adjusted as required to achieve a uniform relative density in each layer. After confirming the target relative density, the specimen was assembled within the triaxial cell.

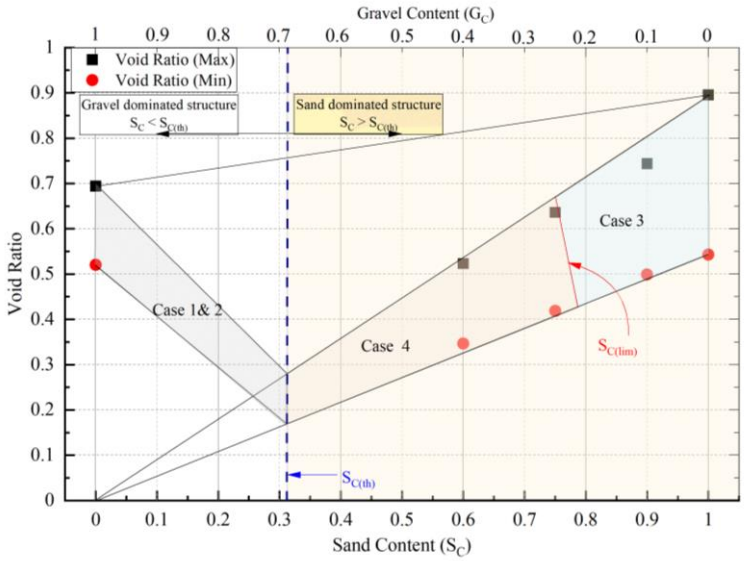

Figure 3 Diagram of microstructure attained for the tested SGMs

After each specimen was placed into the triaxial cell, the cell pressure was increased to 20 kPa and subsequently the specimens were percolated with carbon dioxide for about an hour replacing any air bubble trapped inside the specimen. In the second stage of the saturation process, deaired water was circulated through the specimen at a differential head of 5 kPa by keeping the specimen at constant effective stress of 20 kPa. After percolating deaired water almost double the volume of the specimen, the double vacuum saturation process was initiated by progressively increasing the vacuum pressure in the specimen by 5 kPa steps and maintaining the effective stress at 20 to 25 kPa. The maximum vacuum pressure applied for all the specimens was 80 kPa. After keeping the specimen under the maximum vacuum pressure for at least 2 hours or until the air bubble stopped flowing towards the drainage water tank, the procedure then was inverted.

The specimen was then connected to the triaxial loading system. The cell and back pressures were slowly increased simultaneously with an increment of 50 kPa/10 minutes. In all the tests, Skempton's B values of 0.95 or greater were achieved under a back pressure of 100 kPa. Following, fully saturated specimens were isotropically consolidated up to a 100 kPa confining pressure. Thereafter, stress-controlled undrained cyclic triaxial tests were performed at the frequency of 0.05 Hz using a pneumatic cyclic loading system. The deviatoric stress, effective stress and axial strain were recorded using a built-in data acquisition system.

4 TEST RESULTS AND DISCUSSION

4.1 Test Results

In this study, a series of undrained cyclic tests was carried out on four SGMs (S_C = 0, 10, 25 and 40%) having equal global relative density (D_r = 25 and 45%) to explore the effects of G_C and D_r on the liquefaction resistance of SGMs. The specimens were subjected to cyclic stress ratio (*CSR*) levels ranging between 0.15 and 0.45.

Typical effective stress paths and stress-strain relationships obtained for SGM specimen with G_C = 25% and D_r = 45% subjected to *CSR* = 0.28 are shown in Figure 4 for completeness.

On the other hand, Figure 5 reports the relationships between the *CSR* and number of loading cycles (*N*) to achieve initial liquefaction state or zero effective stress (i.e., r_u = 100%). Interestingly the relationships – here plotted in Log *CSR* – Log *N* scale – are nearly parallel to each other for all SGMs, only shifting upwards with increasing G_C and D_r.

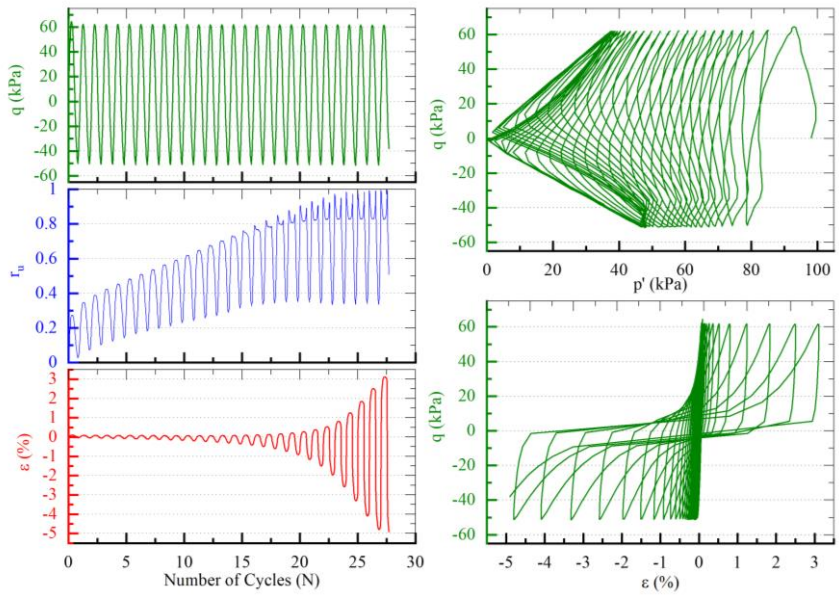

Figure 4 Typical undrained cyclic triaxial behaviour of SGM (G_C = 25%; D_r =45%; CSR = 0.28)

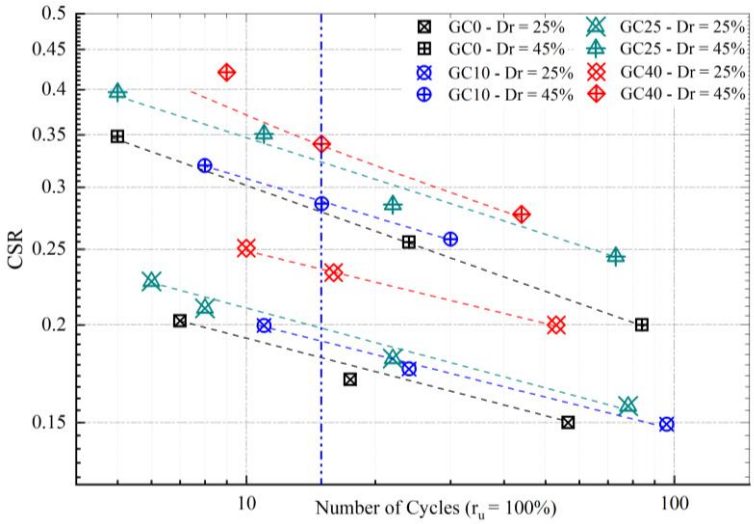

Figure 5 Relationships between CSR and number of loading cycles required to cause initial liquefaction

4.2 Discussion

In this study, the cyclic resistance ratio (*CRR*) of each SGM was defined as the *CSR* value to achieve r_u = 100% in 15 cycles of loading. The variation of *CRR* with G_C at an equal D_r of 25% and 45% is shown in Figure 6. It can be observed that *CRR* marginally increased up to G_C = 25% for the loose specimens and up to G_C = 10% for the medium-dense specimens. This implies that the liquefaction strength is mainly governed by the sand matrix at low D_r and G_C values. However, the *CRR* increases by more than 20% when G_C increases from 25% to 40% in the case of loose specimens and 10% to 40% in the case of medium dense specimens. This is due mainly to the active participation of gravel particles in the sand matrix force chain network affecting the cyclic behaviour of SGMs.

Figure 7 reports the variation of *CRR* with the global void ratio (*e*). The *CRR* increases almost by 55% for G_c = 0, 10 and 40% and by 65% for G_C = 25% when D_r increases from 25 to 45%. The different trend for the G_C = 25% condition can be explained by looking at the inactive and active participation of gravel particles for loose and medium dense specimens. As per the hypothesis aforementioned, the transition zone for gravel

participation in a sand matrix depends on $S_{C(lim)}$. For the tested SGMs, the diagram of microstructure reported in Figure 3 shows that the $S_{C(lim)}$ is nearly equal to S_C at G_C = 25%, when the void ratio is maximum and $S_{C(lim)}$ is about 4% higher than S_C for the minimum void ratio condition. This implies that the G_C = 25% corresponds to the transition zone between active and inactive participation of gravel particles in the sand force chain network.

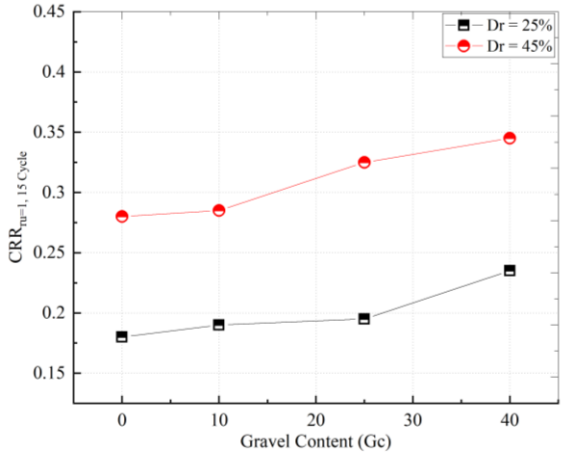

Figure 6 Change in CRR with gravel content at an equal relative density

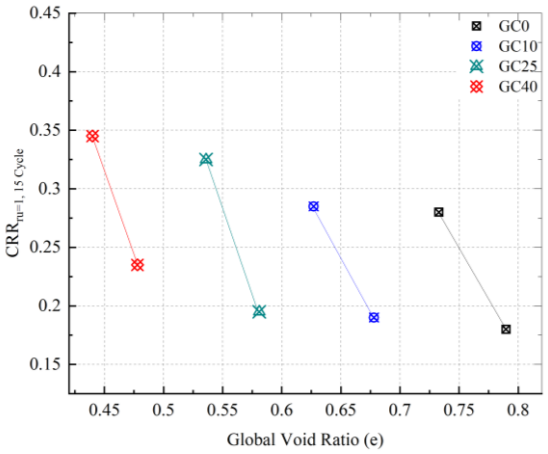

Figure 7 Change in CRR with global void ratio for different SGMs

Figure 7 clearly indicated that the *CRR* of SGMs cannot be uniquely described by the global void ratio (*e*). In the endeavour to search for a more suitable physical state parameter, in this study the relation of *CRR* with skeleton (e_f^*) and equivalent void ratio ($e_{f(eq)}$) were also analysed. The e_f^* was calculated using Eqn. 3, which neglect the effect of gravel particles in the sand matrix. The e_f^* - *CRR* relationship appears to be more promising than that with global void ratio (*e*). Yet, the datapoints are still scattered as shown in Figure **8**.

Figure 9 shows the *CRR* datapoints plotted against the $e_{f(eq)}$. The $e_{f(eq)}$ was calculated using Eqns. 3 and 6. The contact index parameter '*m*' for Eqn. 6 was estimated as 0.7 (based on R^2 method). It is evident that the *CRR* of SGMs can be more precisely and uniquely described by $e_{f(eq)}$, capturing simulatenously both the effects of G_C and D_r.

5 CONCLUSION

A series of undrained cyclic tests was conducted on four selected sand-gravel mixtures (SGMs) to understand the combined effects of the gravel content (G_C) and density state (i.e. relative density, D_r) on the liquefaction resistance of SGMs and to establish a more suitable framework to uniquely describe the *CRR* of SGMs.

The following main conclusions can be drawn from this experimental study:

- *CRR* of SGMs increases with increasing both G_C and D_r. But the effect of G_C and D_r would be marginal to significant depending on the amount of G_C and the D_r of the specimen. This is in a good agreement with relevant previous studies;
- Yet, as suggested by this study, the effects of G_C and D_r on the liquefaction potential of SGMs cannot be considered independently, but should be seen as a combined effect. To this regard, this

study indicates that the equivalent void ratio $e_{f(eq)}$ is a promising parameter to uniquely describe the liquefaction potential of SGMs, since it makes possible to suitably combine the effects of G_C and D_r.

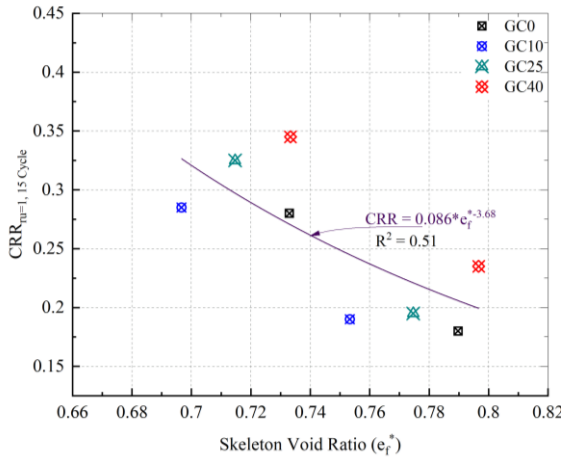

Figure 8 Change in CRR with skeleton void ratio

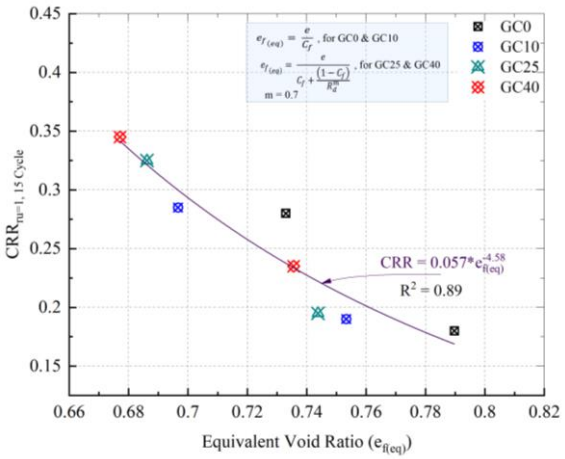

Figure 9 Change in CRR with equivalent void ratio

6 REFERENCES

Amini, F., and Chakravrty, A. 2003. 'Liquefaction Testing of Layered Sand-Gravel Composites'. *Geotechnical Testing Journal*, 27(1), 36–46.

Berrill, J. B., Bienvenu, V., and Callaghan, M. W. 1988. 'Liquefaction in Buller Region 1929 and 1969 Berrill and others.pdf'. *Bulletin of the New Zealand Society for Earthquake Engineering*, 21(3).

Chang, W. J., Chang, C. W., and Zeng, J. K. 2014. 'Liquefaction characteristics of gap-graded gravelly soils in K0 condition'. *Soil Dynamics and Earthquake Engineering*, Elsevier, 56, 74–85.

Chang, W. J., and Phantachang, T. 2016. 'Effects of gravel content on shear resistance of gravelly soils'. *Engineering Geology*, 207, 78–90.

Chen, G., Wu, Q., Sun, T., Zhao, K., Zhou, E., Xu, L., and Zhou, Y. 2018. 'Cyclic Behaviors of Saturated Sand-Gravel Mixtures under Undrained Cyclic Triaxial Loading'. *Journal of Earthquake Engineering*, 2469.

Cubrinovski, M. 2019. 'Some important considerations in the engineering assessment of soil liquefaction'. *NZ Geomechanics News*, (97).

Cubrinovski, M., Bray, J. D., De La Torre, C., Olsen, M. J., Bradley, B. A., Chiaro, G., Stocks, E., and Wotherspoon, L. 2017. 'Liquefaction effects and associated damages observed at the Wellington centreport from the 2016 Kaikoura earthquake'. *Bulletin of the New Zealand Society for Earthquake Engineering*, 50(2), 152–173.

Cubrinovski, M., Green, R. A., Allen, J., Ashford, S., Bowman, E., Brendon, Bradley, Cox, B., Hutchinson, T., Kavazanjian, E., Orense, R., Pender, M., Quigley, M., and Wotherspoon, L. 2010. 'Geotechnical reconnaissance of the 2010 Darfield (Canterbury) earthquake'. *Bulletin of the New Zealand Society for Earthquake Engineering*, 43(4), 243–320.

Evans, M. D., and Zhou, S. 1995. 'Liquefaction behavior of sand-gravel composites'. *Journal of Geotechnical Engineering*, 121(3), 287–298.

Ishihara, K. (1993). 'Liquefaction and flow failure during earthquakes'. *Geotechnique*, 43(3), 351–451.

Kokusho, T., Hara, T., and Hiraoka, R. 2004. 'Undrained Shear Strength of Granular Soils with Different Particle Gradations'. *Journal of Geotechnical and Geoenvironmental Engineering*, 130(6), 621–629.

Mitchell, J. K., and Soga, K. 1994. *Fundamentals of Soil Behavior*. *Soil Science*.

Rahman, M. M., Lo, S. R., and Gnanendran, C. T. 2008. 'On equivalent granular void ratio and steady state behaviour of loose sand with fines'. *Canadian Geotechnical Journal*, 45(10), 1439–1456.

Rahman, M. M., Lo, S. R., and Gnanendran, C. T. 2009. 'Reply to the discussion by wanatowski and chu on "on equivalent granular void ratio and steady state behaviour of loose sand with fines"'. *Canadian Geotechnical Journal*, 46(4), 483–486.

Thevanayagam, S. 1998. 'Effect of Fines and Confining Stress on Undrained Shear Strength of Silty Sands'. *Journal of Geotechnical and Geoenvironmental Engineering*, 124(6), 479–491.

Thevanayagam, S. 2000. 'Liquefaction potential and undrained fragility of silty soils'. *Proceedings of the 12th World Conference on Earthquake Engineering*, 1–8.

Thevanayagam, S. 2007. 'Intergrain contact density indices for granular mixes - I: Framework'. *Earthquake Engineering and Engineering Vibration*, 6(2).